acetone in deoxycholic acid. We are presently using these techniques to elucidate the influence of solvent order on Norrish II photoreactions of ketones in the solid and rotator phases of alkanes[32] and in the ordered phases of *trans,trans*-4-butylbicyclohexyl-4′-carbonitrile.[38]

(37) Meirovitch, E. *J. Phys. Chem.* **1986**, *90*, 5825.
(38) Treanor, R. L.; Weiss, R. G. *J. Phys. Chem.* **1987**, *91*, 5552.

Acknowledgment. We thank the National Science Foundation (Grant CHE85-17632) for support of this work. The W. M. Keck Foundation provided an instrument grant. We thank Dr. J. Michael Geckle of Bruker Instruments, Inc., and Dr. Charles Hammer of Georgetown for their assistance at the inception of the ^2H NMR studies, and Dr. Dennis Torchia of the National Institutes of Health for helpful discussions. Mrs. Patricia Vilalta provided the KP data at 15 °C.

Chiral Discotic Columnar Mesophases from the α and β Anomers of Penta-*O*-*n*-alkanoylglucopyranoses[1]

Nancy L. Morris, Richard G. Zimmermann,† Geoffrey B. Jameson,* Adam W. Dalziel, P. Matthew Reuss,‡ and Richard G. Weiss*

Contribution from the Department of Chemistry, Georgetown University, Washington, D.C. 20057. *Received August 10, 1987*

Abstract: The detailed phase behavior of the α and β anomers of penta-*O*-*n*-alkanoylglucopyranoses (α- and β-G_n, where *n*, the number of carbons in each alkanoyl chain, is 10–16 or 18) has been investigated by differential scanning calorimetry, X-ray diffraction, optical microscopy, and circular dichroism. All members of both anomeric series form at least one columnar discotic mesophase. The shorter chained α anomers, especially, give rise to a reentrant solid phase upon slow heating of their mesophases. The same molecules pack helically in columns with 6 molecules completing a full twist. No evidence was obtained for rotational ordering of molecules within columns of the longer chained α-G_n or β-G_n. However, shorter homologues of both series appear to form columns whose total shapes may become twisted. The thermal histories of samples, in terms of both their duration at one temperature and their rates of heating or cooling, determine the packing arrangements and (to a lesser extent) the heats of transition. A detailed discussion of the phases and the factors responsible for their formation is presented.

The unifying feature of all columnar mesophases is the shape of the individual constituent molecules.[2] Whereas most nematic, smectic, and cholesteric molecules are somewhat cylindrical, discotic molecules (as their name implies) are relatively flat and coin-shaped.[3,4] Most known mesomorphic discotic molecules consist of a rigid, aromatic core symmetrically surrounded by 6–8 substituent chains.[5] Recently, we discovered a new class of mesomorphic discotic molecules which are peralkanoylated cyclic mono- and disaccharides. Their cores are nonaromatic, unsymmetrical, and chiral. In a preliminary communication, we reported on the mesomorphic properties of two examples, the α and β anomers of penta-*O*-*n*-decanoylglucopyranose (α- and β-G_{10}).[6] Here, we describe in detail the homologous series of anomeric peralkanoylated glucopyranoses (α- and β-G_n, where n = 10–16, 18) for which each molecule contains only 5 chains. Since the G_n are prepared in one step from commerically available, inexpensive reagents, they can be obtained easily in large quantities.

Smectic mesophases of cyclic saccharides that are monosubstituted at the anomeric carbon are well documented.[7] The report nearly 50 years ago that tetraacetyl alkylglucopyranosides do not exhibit a mesophase[8] may have dissuaded others from seeking liquid crystallinity in longer pentaacylated glucopyranosides. In fact, several α- and β-G_n have been synthesized in the interim.[9] A careful reading of the original literature[9a] does allow one, in retrospect, to suspect that they are mesomorphic. In spite of this, the prevalent view is that compounds like α- and β-G_n are not.[10]

The closest relatives of the G_n are the peralkanoylated inositols prepared by Kohne and Praefcke.[11] Like the peralkanoylated *myo*-inositols (**1**), the α-G_n have one axial substituent (at the anomeric carbon). Like the *scyllo*-inositols (**2**), the β-G_n have only equatorial substituents when the glucopyranose ring is in a chair-like conformation.

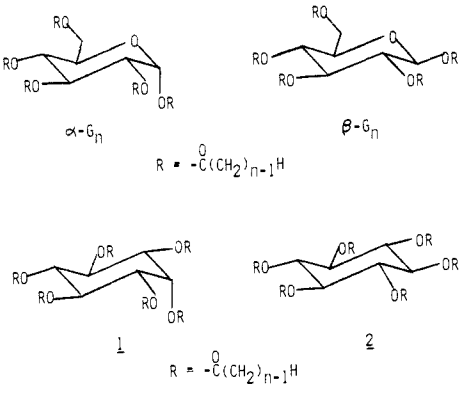

* Authors to whom inquiries should be sent.
† Present address: CRES-SOBIO, Saint Gregoire, France.
‡ Summer research participant from Reed College, Portland, OR.

(1) Part 29 in our series "Liquid-Crystalline Solvents as Mechanistic Probes". For part 28, see: Treanor, R. L.; Weiss, R. G. *J. Phys. Chem.* **1987**, *91*, 5552.
(2) (a) Chandrasekhar, S.; Sadashiva, B. K.; Suresh, K. A. *Pramana* **1977**, *9*, 471. (b) Chandrasekhar, S.; Sadashiva, B. K.; Suresh, K. A.; Madhusudana, N. V.; Kumar, S.; Shashidhar, R.; Venkatesh, G. *J. Phys.* (*Les Ulis, Fr.*) **1979**, *40*, C3–120.
(3) See, for instance: (a) Dubois, J. C.; Billard, J. In *Liquid Crystals and Ordered Fluids*; Griffin, A. C., Johnson, J. F., Eds.; Plenum: New York, 1984; Vol. 4, p 1043. (b) Destrade, C.; Gasparoux, H.; Foucher, P.; Tinh, N. H.; Malthete, J.; Jacques, J. *J. Chim. Phys.* **1983**, *80*, 137. (c) Chandrasekhar, S. In *Advances in Liquid Crystals*; Brown, G. H., Ed.; Academic: New York, 1982; Vol. 5, p 47.
(4) Some cylindrical lyotropic molecules can aggregate in radially dispersed subunits which appear discotic.[4a–c] Dimers of others form discotic phases also.[4d] (a) Acimis, M.; Reeves, L. W. *Can. J. Chem.* **1980**, *58*, 1542. (b) Fujiwara, F. Y.; Reeves, L. W. *Can. J. Chem.* **1980**, *58*, 1550. (c) Spegt, P. A.; Skoulios, A. *Acta Crystallogr.* **1966**, *21*, 892. (d) Bunning, J. D.; Lydon, J. E.; Eaborn, C.; Jackson, P. M.; Goodby, J. W.; Gray, G. W. *J. Chem. Soc., Faraday Trans. 1* **1981**, *78*, 713.

0002-7863/88/1510-2177$01.50/0

Careful optical microscopy (OM), differential scanning calorimetry (DSC), and X-ray diffraction studies have disclosed several intriguing aspects of the mesomorphic glucopyranoses: (1) a number of the lower homologues exhibit *reentrant solid* phases;[12] (2) some members of the series may form more than one mesophase; (3) the packing arrangements of the lower homologues of α-G_n (n = 10, 11), the higher homologues ($n \geq 12$), and the β-G_n are distinctly different but are clearly columnar; (4) some G_n retain memories of their prior thermal histories. The above properties and the lack of chromophores absorbing in the near-ultraviolet region make α-G_n and β-G_n well suited as ordered solvents in which spectroscopic and mechanistic studies[13] (our original impetus for this work) can be made. Although, they appear to be monotropic, many of the G_n have very long-lived mesophases.

Experimental Section

High-performance liquid chromatography (HPLC) was performed on a Waters instrument equipped with both ultraviolet (254 nm) and refractive index detectors. All compounds were analyzed on a Waters Rad-Pak B silica column (10 μm) and 5/95 ethyl acetate/hexane as eluent at 2.5 cm^3/min. Melting points and transition temperatures, obtained on a Kofler micro hot-stage microscope equipped with plane light polarizers, are corrected. Infrared absorption spectra in chloroform solutions were recorded on a Perkin-Elmer 457 or a Sargent-Welch spectrophotometer. Proton NMR spectra were obtained with a Bruker AM300WB spectrometer using an Aspect 3000 computer, and resonances were referenced to internal tetramethylsilane. Optical rotations were measured on a Perkin-Elmer 241 electronic polarimeter in 1-dm-length fused-quartz tubes. Column chromatography by the flash method[14] used silica (Merck Kieselgel 60 or Baker 60–200 mesh.)

Elemental analyses were performed by Galbraith Laboratories, Knoxville, TN.

X-ray Diffraction Experiments. Diffraction data were measured on a Picker powder diffractometer with Ni-filtered Cu Kα radiation (1.5418 Å), Soller collimators, and a 0.002-in. receiving aperture. The samples were placed in a temperature-controlled aluminum block with an oval depression for sample containment. Temperature measurement was provided by a thermocouple placed in the block. The sample farthest from the thermocouple varied in temperature by ca. 0.5 °C from material nearest it. Nitrogen was blown over the sample at lower temperatures to prevent water condensation. Some problems were encountered in early diffraction measurements due to a peak attributed to amorphous aluminum which occurred around 10° in 2θ and grew with time. Later, the artifact was eliminated by electroplating the holder with copper. In another experiment, a sample of α-G_{10} was placed in a 1-mm-diameter, thin-walled (0.01 mm) capillary, and the liquid-crystalline phase was studied on a Picker FACS-1 four-circle diffractometer with NRC-Canada software (from E. Gabe) with Mo radiation (0.7107 Å); slow θ–2θ step scans were used. Sample uniformity was checked by scans with χ = 0° and 270° and ϕ = 0° and 90°. Some preferential orientation was detected. In addition, a sample of β-G_{16} was run with a mica standard as internal reference on the powder diffractometer. Both methods indicated a correction factor of 0.40° for 2θ values for the powder diffractometer. We have therefore used the adjusted 2θ values.

Selected samples, oriented on very thin glass plates, were examined on the Nicolet P2$_1$ diffractometer using graphite-monochromated Mo Kα radiation and Polaroid film to sample the diffraction pattern in two dimensions.

Materials. α-Glucose and β-glucose (Sigma), containing ca. 5% and 2% of the other anomer, respectively, were used as received. Undecanoyl chloride, tridecanoyl chloride, and pentadecanoyl chloride were obtained from the corresponding acids (Aldrich) by refluxing them for 30 min in a large excess of freshly distilled thionyl chloride containing a drop of dimethylformamide. Each acyl chloride was distilled before use: undecanoyl chloride, bp 90–95 °C (1 Torr); tridecanoyl chloride, bp 119 °C (1.6 Torr); pentadecanoyl chloride, bp 128 °C (1.2 Torr). Penta-acetyl-α- and -β-glucopyranoses were used as received from Sigma.

Preparation of Penta-*n*-alkanoylglucopyranoses. In a typical experiment, 5 mmol of sugar was stirred at room temperature in a mixture of 5 mL of dry pyridine (Baker) and 30 mL of chloroform (Baker, alcohol free.) A solution of 30–40 mmol of acyl chloride in 10 mL of chloroform was added slowly, and the mixture was stirred in a closed vessel for 24–72 h or until the solid had disappeared.[15a] The residue that remained after solvent removal on a rotary evaporator was dissolved in 100 mL of methylene chloride. It was extracted sequentially with 30 mL of 5% aqueous H_2SO_4, 3 × 30 mL of 5% aqueous NaOH,[15b] 30 mL of 5% aqueous H_2SO_4, 30 mL of saturated aqueous $NaHCO_3$, and 30 mL of a saturated salt solution. The organic layer was dried (anhydrous $MgSO_4$) and evaporated carefully to residue. The crude product was flash chromatographed and recrystallized. At this point, yields usually were 60–90%. Recrystallizations or precipitations (Table I) were performed until only one peak could be noted by HPLC (refractive index detection.) Physical constants for the products are collected in Table II. Elemental analyses were performed on compounds that have not been reported previously, except β-G_{10} and β-G_{16}, which were recently made and analyzed by Kohne and Praefcke.[11] All of the samples, except α-G_{12}, gave only one peak by HPLC after purification.

Calorimetry. Calorimetry was conducted with a Perkin-Elmer DSC-7 differential scanning calorimeter equipped with a thermal analysis data station and an intercooler. Sample pans consisted of a three-part (pan, cover, and O-ring) hermetically sealed stainless steel assembly. Samples typically contained 10–20 mg of material, and the reference pans were empty. Heating and cooling rates of 0.5 °C/min were used unless specified otherwise. The peak temperatures for the endotherm and ex-

Table I. Recrystallization Procedures for Purification of G_n

compd	recrystallization procedure
α-G_{10}	hexane (2×), isopropyl alcohol
α-G_{11}	isopropyl alcohol (3×)
α-G_{12}	isopropyl alcohol (3×)
α-G_{13}	isopropyl alcohol (3×), hexane, 1/1 chloroform/ethanol
α-G_{14}	isopropyl alcohol (3×), hexane (2×)
α-G_{15}	isopropyl alcohol (3×)
α-G_{16}	isopropyl alcohol (3×), hexane, 1/1 chloroform/ethanol (2×), acetone
α-G_{18}	hexane (2×), 1/5 chloroform/acetone
β-G_{10}	hexane (2×), isopropyl alcohol
β-G_{11}	isopropyl alcohol (3×)
β-G_{12}	isopropyl alcohol (3×)
β-G_{13}	isopropyl alcohol (3×)
β-G_{14}	isopropyl alcohol (3×)
β-G_{15}	isopropyl alcohol (3×)
β-G_{16}	isopropyl alcohol (3×)
β-G_{18}	hexane (2×)

(5) (a) Takenaka, S.; Nishimura, K.; Kusabayashi, S. *Mol. Cryst. Liq. Cryst.* **1984**, *111*, 227. (b) Nishimura, K.; Takenaka, S.; Kusabayshi, S. *Mol. Cryst. Liq. Cryst.* **1984**, *104*, 347. (c) Malthete, J.; Collet, A. *Nouv. J. Chim.* **1985**, *9*, 151. (d) Zimmermann, H.; Poupko, R.; Luz, Z.; Billard, J. *Z. Naturforsch., A* **1985**, *40a*, 149. (e) Malthete, J.; Levelut, A.-M.; Tinh, N. H. *J. Phys. (Les Ulis, Fr.)* **1985**, *46*, L875. (f) Lehn, J.-M.; Malthete, J.; Levelut, A.-M. *J. Chem. Soc., Chem. Commun.* **1985**, 1794. (g) Kok, D. M.; Wynberg, H.; de Jeu, W. H. *Mol. Cryst. Liq. Cryst.* **1985**, 129, 53. (h) Fugnitto, R.; Strzelecka, H.; Zann, A.; Dubois, J. C. *J. Chem. Soc., Chem. Commun.* **1980**, 271.

(6) Zimmermann, R. G.; Jameson, G. B.; Weiss, R. G.; Demailly, G. *Mol. Cryst. Liq. Cryst., Lett.* **1985**, *1*, 183.

(7) (a) Barrall, E.; Grant, B.; Oxsen, M.; Samulski, E. T.; Moews, P. C.; Knox, J. R.; Baskill, R. R.; Haberfeld, J. L. *Org. Coat. Plast. Chem.* **1979**, *40*, 67. (b) Goodby, J. W. *Mol. Cryst. Liq. Cryst.* **1984**, *110*, 205. (c) Lejay, J.; Pesquer, M. *Mol. Cryst. Liq. Cryst.* **1984**, *111*, 293. (d) Jeffrey, G. A. *Mol. Cryst. Liq. Cryst.* **1984**, *110*, 221. (e) Koll, P.; Oelting, M. *Tetrahedron Lett.* **1986**, *27*, 2837. (f) Jeffrey, G. A. *Acc. Chem. Res.* **1986**, *19*, 168. (g) Pfannemuller, B.; Welt, W.; Chin, E.; Goodby, J. W. *Liq. Cryst.* **1986**, *1*, 357. (h) Jeffrey, G. A.; Bhattacharjee, S. *Carbohydr. Res.* **1983**, *115*, 53. (i) Marcus, M. A.; Finn, P. L. *Mol. Cryst. Liq. Cryst., Lett.* **1985**, *2*, 159.

(8) Noller, C. R.; Rockwell, W. C. *J. Am. Chem. Soc.* **1938**, *60*, 2076.

(9) (a) Zemplen, G.; Laszlo, E. D. *Ber.* **1915**, *48*, 915. (b) Hess, K.; Messmer, E. *Ber.* **1921**, *54B*, 499. (c) Voitenko, A. V.; Volkova, L. V.; Evstigneeva, R. P. *J. Gen. Chem. USSR (Engl. Transl.)* **1980**, *50*, 137.

(10) In 1986, Jeffrey[7f] wrote of carbohydrates: "Hitherto, there are no examples of mesogens with more than one alkyl chains." Kohne and Praefcke[11] reported that α-G_{10}, β-G_{10}, α-G_{18}, and β-G_{18} are not mesogenic.

(11) (a) Kohne, B.; Praefcke, K. *Chem. Ztg.* **1985**, *109*, 121. (b) Kohne, B.; Praefcke, K. *Abstracts*, X International Liquid Crystal Congress, Hull, England, July 1984; Abstract H17. (c) Kohne, B.; Praefcke, K. *Angew. Chem., Int. Ed. Engl.* **1984**, *23*, 82.

(12) Somewhat related behavior has been found in neat phases of disk-shaped Cu(II) complexes: (a) Ohta, K.; Muroki, H.; Hatoda, K.-I.; Yamamoto, I.; Matsuzaki, K. *Mol. Cryst. Liq. Cryst.* **1985**, *130*, 249. (b) Ohta, K.; Ema, H.; Muroki, H.; Yamamoto, I.; Matsuzaki, K. *Mol. Cryst. Liq. Cryst.* **1987**, *147*, 61.

(13) See, for instance: (a) Zimmermann, R. G.; Liu, J. H.; Weiss, R. G. *J. Am. Chem. Soc.* **1986**, *108*, 5264. (b) Ramesh, V.; Weiss, R. G. *J. Org. Chem.* **1986**, *51*, 2535. (c) Anderson, V. C.; Weiss, R. G. *J. Am. Chem. Soc.* **1984**, *106*, 6628. (d) Ganapathy, S.; Zimmermann, R. G.; Weiss, R. G. *J. Org. Chem.* **1986**, *51*, 2529.

(14) Still, W. C.; Kahn, M.; Mitra, A. *J. Org. Chem.* **1978**, *43*, 2923.

(15) (a) The reaction time can be reduced to a few hours by refluxing the mixture in a dry atmosphere. (b) Foams or emulsions were noted in some preparations at this stage. They were destroyed by adding small amounts of aqueous H_2SO_4 and maintaining the pH > 10.

Table II. Physical and Spectroscopic Data for α-G_n and β-G_n

compd	elem anal. calcd % C	calcd % H	found % C	found % H	IR ($CHCl_3$), cm^{-1}	HPLC[a] ret time, min	$[\alpha]^{21-22}(CHCl_3)$, deg
α-G_9					1740	*b*	+39.2
α-G_{10}					1755	4.3	+44.0 (+42.0[e])
α-G_{11}	71.72	11.05	71.68	10.65	1740	3.4	+38.3
α-G_{12}					1739	3.1	+43.6 (+40.62[f])
α-G_{13}	73.40	11.45	73.30	11.68	1740	3.0	+40.8
α-G_{14}	74.10	11.62	74.39	11.20	1740	2.9	+36.5
α-G_{15}	74.72	11.77	74.31	11.82	1745	2.9	+35.4
α-G_{16}					1745	2.4	+30.2 (+29.7,[f] +33,[e] +34.3[g])
α-G_{18}					1755	2.6	+30.2 (+32.8,[e] +34.2[g])
β-G_9							
β-G_{10}	70.69	10.81	70.81	10.62	1740	*b*	+7.1
β-G_{11}	71.72	11.05	72.01	10.82	1740	*b*	*b*
β-G_{12}	73.19	11.37	72.90	11.53	1760[c]	2.8	+5.9 (+6.1[h])
β-G_{13}	73.40	11.45	73.38	11.66	1745	4.5	+5.7
β-G_{14}	74.10	11.62	74.32	11.62	1739	6.0	+5.3 (+3.9[f])
β-G_{15}	74.72	11.77	74.62	11.40	1749	5.1	+4.4
β-G_{16}					1740[d]	3.2	+8.7 (+4.0,[h] +4.6[f])
β-G_{18}					1760	3.2	+3.8 (+14.1[f])

[a] See Experimental Section for details. [b] Not determined. [c] Lit.[11a] 1759 cm^{-1}. [d] Lit.[11a] 1757 cm^{-1}. [e] Reference 9c. [f] Reference 9a. [g] Reference 9b. [h] Reference 11a.

Table III. Transition Data for α-G_n and β-G_n from DSC Measurements (First and Second Heating Scans)[a]

compd	temp,[b] °C scan 1	scan 2	lit.	enthalpy,[c] J/g scan 1	scan 2
α-G_9	<25[d]				
α-G_{10}	35.6	32.6	27–28[e]	52.1	31.2
α-G_{11}	49.2	44.3		74.5	68.4
α-G_{12}	51.3	46.1	48–52[f]	109.0	94.8
α-G_{13}	58.2	57.9		89.4	74.7
α-G_{14}	57.7	58.3		99.5	100.5
α-G_{15}	59.5	59.4		106.2	102.6
α-G_{16}	68.0	67.8	65–66,[e] 65–67,[g] 62[h]	107.8	104.5
α-G_{18}	73.6	73.0	71–72,[e] 70–71[g]	116.5	108.0
β-G_9	<25[d]				
β-G_{10}	39.7	34.0	38–39[i]	65.1	56.0
β-G_{11}	46.8	46.4		71.4	69.1
β-G_{12}	52.6	52.5	60–66[f]	79.8	75.6
β-G_{13}	60.9	60.4		83.2	80.4
β-G_{14}	65.6	66.1		86.6	86.7
β-G_{15}	70.5	69.9		95.7	92.3
β-G_{16}	75.2	74.4	67–72,[f] 72.5–73.5[i]	96.6	109.3
β-G_{18}	79.9	79.5	72–78[f]	106.4	102.7

[a] The first scans employ material purified as described in Table I and may contain solid, mesophase, or a mixture of the two. [b] ±0.5 °C. [c] ±2%. [d] By OM. [e] Reference 9c. [f] Reference 9a. [g] Reference 9b. [h] Stephenson, M. *Biochem. J.* **1913**, *7*, 429. [i] Reference 11a.

otherm in heating and cooling scans, respectively, were recorded. A correction factor derived from the difference between the observed peak temperatures and the true indium melting temperature (156.6 °C), regularly monitored as a calibration standard, was then applied to the transitions for heating and cooling scans, respectively. Transition data from the first and second heating scans (0.5 °C/min) for α-G_n and β-G_n are collected in Table III. Differences are a result of the mixed morphologies obtained upon precipitation (Table I). The accuracy of the results presented is estimated to be 0.5 °C.

Optical Rotary Dispersion and Circular Dichroism Spectra. A 0.12% solution of pyrene in β-G_{10} was prepared by heating and mixing the two compounds together and then allowing the solution to cool. An aliquot was sandwiched between two quartz plates separated by a 25-μm Teflon spacer, and the plates were placed in a thermostated holder. After 18 h at room temperature, the holder was placed in the sample compartment of a JASCO ORD/5 with a CD attachment. The sample was temperature equilibrated, and spectra were recorded without moving the thermostating compartment. ORD spectra were recorded for chloroform solutions of several members of the α and β series. All were plane positive curves between 600 and 400 nm.

Results and Discussion

Chemical Identification and Purity of α- and β-G_n. The chemical identity of α-G_n and β-G_n was confirmed by several techniques.

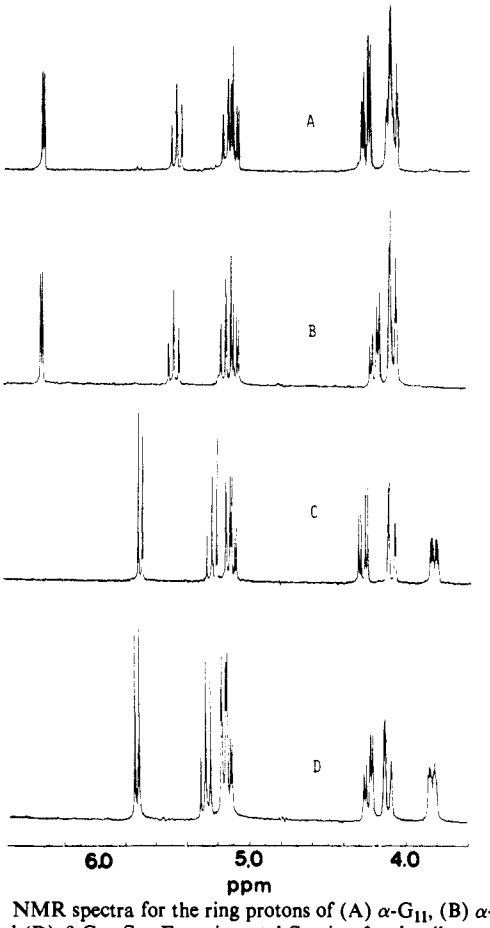

Figure 1. NMR spectra for the ring protons of (A) α-G_{11}, (B) α-G_2, (C) β-G_{11}, and (D) β-G_2. See Experimental Section for details. α-G_{11} and β-G_{11} give typical spectra of their respective homologous series. Note the presence of a detectable amount of β-anomeric peaks at 3.8 and 5.7 ppm in the α spectra and the absence of any α-anomeric peak (especially at 6.35 ppm) in the β spectra, in accordance with our assignments of purity.

The most conclusive of these were the known synthetic method[16] and 300-MHz proton magnetic resonance spectrometry. The presence of the glucopyranose ring was evident in the α-G_n and β-G_n from comparisons of the chemical shifts, splitting patterns,

(16) See, for instance: Ames, G. R. *Chem. Rev.* **1960**, *60*, 541 and references cited therein.

and intensities of the low-field proton resonances (see Figure 1) with those of authentic samples of α-G_2 and β-G_2.[17]

The similarity among the G_n does not allow elemental analyses, optical rotations, etc. (see Table II) to serve as precise measures of structural purity. HPLC analyses, especially when combined with the NMR spectra, do permit a lower limit on purities to be determined. All samples used for DSC measurements (except α-G_{12}) showed only one peak by refractive index detection. The similarity of the retention volumes of many of the G_n and the relative insensitivity of this detector led us to believe that as much as 5% of an impurity (with an equal detector response) could have been present. The impurities in the G_n arise from the reagent acyl chlorides containing small amounts of homologues and each glucopyranose containing some of the other anomer. While small amounts of impurities do undoubtedly slightly alter batch-to-batch phase transition temperatures, they cannot account for the mesomorphism and reentrant behavior, which we describe in the next sections.

In almost all cases, X-ray and OM measurements were performed on aliquots from the same or an equally pure batch. Samples were usually dried at slightly elevated temperatures in a vacuum oven prior to their use in order to remove traces of solvents of recrystallization: some homologues appeared to form weak complexes with alcohol. Compounds purified in this fashion had the appearance of soft, white solids. Both OM and DSC indicated that the solids consisted of mixtures of crystals and mesophase. For this reason the second heating scan data of Table III are a more accurate measure of the mesophase-to-isotropic transition characteristics. Subsequent melting and cooling produced crystal, mesophase, or a mixture of the two depending upon the details of the thermal cycles.

The data in Table III are incompatible with a crystalline–isotropic phase transition: for linear polyethylene, Billmeyer[18] calculates the heat of fusion to be 275 J/g. They do not follow the trends expected for cholesteric–isotropic or smectic cholesteryl *n*-alkanoates[19] and cholesteryl ω-phenylalkanoates.[20] For instance, the per-gram heats of transition from α- or β-G_n are 20–30 times greater in magnitude than those from the cholesteric–isotropic transitions of 5α-cholest-8(14)-en-3β-yl alkanoates.[21] They also exceed by similar amounts the per-gram heats of transition (mesophase–isotropic) for discotic triphenylenehexayl hexa-*n*-alkanoates[22] and benzenehexayl hexa-*n*-alkanoates.[2a] The per-gram heats of transition to the isotropic phase for **2**, however, are only slightly larger than those of the analogous β-G_n.[23] The trends in the per-gram heats of transition differ: whereas the heats for both the triphenylenes and **1** decrease as the ester chain lengths increase, the heats from G_n increase with longer chains and appear to approach a plateau value in the α-anomeric series. The greatest increases between α homologues occur between α-G_{10}, α-G_{11}, and α-G_{12}. As will be discussed later, the α-G_{10} and α-G_{11} appear to pack differently than the other α-G_n ($n \geq 12$). Except for β-G_{18}, the second heating scans of the β anomers produce per-gram endotherms that increase at a nearly constant value (ca. 15 J/g) between homologues. For neither series have we chosen to calculate entropies of transition since cooling curves exhibit extensive supercooling prior to the exotherm peak.

Determination of Phase Types: Liquid Crystal Induced Circular Dichroism (LCICD) Observations:[24] Evidence for Twisted Columnar Organization. In the isotropic phase, a dilute 25-μm-thick solution of pyrene (0.12% by weight) in β-G_{10} displayed no perceptible circular dichroism between 500 and 280 nm (Figure 2A)—nor did a sample of neat β-G_{10} at 32 °C. After the sample was incubated at room temperature (ca. 28 °C) overnight, characteristic dichroic bands of pyrene appeared at 338, 331, 319, and 305 nm (Figure 2B). Further spectra recorded in rapid succession at 11, 17, and 28 °C were indistinguishable from Figure 2B. Heating to 42 °C resulted in the loss of LCICD. When the sample was rapidly cooled (several seconds) from the isotropic phase to 19 °C, the pyrene peaks were not apparent in the circular dichroism spectrum. Reheating to the isotropic phase followed by slow cooling to room temperature (28 °C) and overnight incubation resulted in a much stronger dichroic absorption for the pyrene transitions (Figure 2C). Similar results were obtained with a solution of 0.6% (by weight) pyrene in α-G_{10}. A spectrum taken at T = 21 °C, after incubating the sample at 0 °C for 60 h and then warming slowly, is shown in Figure 2D.

Our inability to align samples consistently or to obtain isotropic spectra that have the same initial absorption makes quantitative analyses of these data unwise. However, the weakness of the initial dichroic spectra from rapidly cooled samples especially is consistent with a first-formed homeotropic alignment of the phases.

The presence of LCICD indicates a macrohelical arrangement of the discotic molecules in their mesophase. However, attempts to locate a pitch band,[25] characteristic of the periodicity of twist,

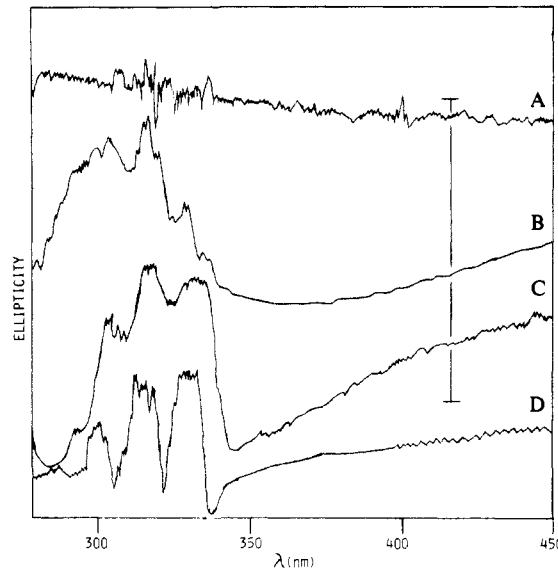

Figure 2. Liquid crystal induced circular dichroism spectra of pyrene in α-G_{10} and β-G_{10}. Pyrene (0.12%) in β-G_{10} at (A) 38, (B) 28, and (C) 28.5 °C; (D) 0.6% pyrene in α-G_{10} at 21 ± 1 °C. See Results and Discussion for details. The vertical line represents 0.001° of ellipticity for (A) and (D) and 0.0004° for (B) and (C).

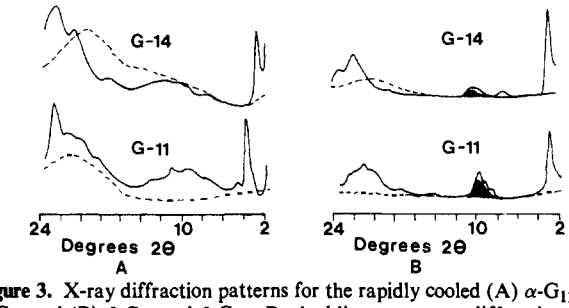

Figure 3. X-ray diffraction patterns for the rapidly cooled (A) α-G_{11} and α-G_{14} and (B) β-G_{11} and β-G_{14}. Dashed lines represent diffraction from the isotropic sample. Darkened areas are diffraction attributed to Al_2O_3 or amorphous Al. Unless indicated otherwise, T = 15 °C.

(17) *Sadtler Standard Spectra. NMR*; Sadtler Research Laboratories: Philadelphia; Spectra 24737M and 5521M.
(18) Billmeyer, F. W., Jr. *J. Appl. Phys.* **1957**, *28*, 1114.
(19) Emmulat, R. D. *Mol. Cryst. Liq. Cryst.* **1969**, *8*, 247.
(20) Pohlmann, J. L. W.; Elser, W.; Boyd, P. R. *Mol. Cryst. Liq. Cryst.* **1973**, *20*, 87.
(21) Chu, J. Y. C. *J. Phys. Chem.* **1975**, *79*, 119.
(22) Destrade, C.; Mondon, M. C.; Malthete, J. *J. Phys. (Les Ulis, Fr.)* **1979**, *40*, C3.
(23) Kohne, B.; Praefcke, K.; Billard, J. *Z. Naturforsch., B* **1986**, *41b*, 1036.
(24) (a) Saeva, F. D. In *Liquid Crystals. The Fourth State of Matter*; Saeva, F. D., Ed.; Marcel Dekker: New York, 1979; Chapter 6. (b) Ganapathy, S.; Weiss, R. G. In *Organic Transformations in Non-Homogeneous Media*; Fox, M. A., Ed.; American Chemical Society: Washington, DC, 1986; p 142. (c) Anderson, V. C.; Weiss, R. G. *J. Am. Chem. Soc.* **1984**, *106*, 6628.
(25) (a) Baessler, H.; Labes, M. M. *Mol. Cryst. Liq. Cryst.* **1970**, *6*, 419. (b) Fergason, J. L. *Mol. Cryst.* **1966**, *1*, 293. (c) Adams, J.; Haas, W. *Mol. Cryst. Liq. Cryst.* **1972**, *16*, 33.

Table IV. Summary of *d* Values from Film Data Showing Sample Orientation Effects[a]

α-G_{10}		β-G_{10}	
horiz	vert	horiz	vert
meridional	meridional	20 (4) vs	17 (3) vs
20 (4) vs	17 (3) vs	8.6 (6) s	8.6 (6) s
15 (2) m	12 (1) s	3.5 (1) vs	3.4 (1) s
9.3 (7) m	10.1 (9) w		1.81 (3) w
7.1 (4) m	8.0 (6) w		
5.7 (3) w	6.3 (4) m		
4.5 (1) s	4.0 (1) m		
3.8 (1) s	3.34 (9) s		
3.4 (1) s			
2.13 (4) m			
equatorial	equatorial		
17 (3) vs	20 (4) vs		
7.1 (4) m	7.5 (5) w		
3.4 (1) s	4.5 (1) s		
	3.9 (1) s		
	3.4 (1) s		
	2.17 (3) m		

α-G_{16}			β-G_{16}	
horiz	vert	face-on	horiz	vert
12.1 (1) s	12.1 (1) s	12.1 (1)	10.1 (9) s	12 (1) s
3.34 (9) s	8.0 (6) m	3.5 (1)	7.1 (4) s	8.6 (6) s
	3.8 (1) s	1.85 (3)	3.34 (9) s	3.4 (1) s
	3.2 (1) s		1.69 (2) w	
	1.85 (3) m			

[a] Intensities are indicated by a letter following the *d* value: vs = very strong, s = strong, m = medium, w = weak. Film-to-sample distance was 85 (2) mm. Numbers in parentheses are errors in the last digit. Horiz and vert denote orientation of glass slide with respect to X-ray beam. Meridional and equatorial refer to directions on the film.

in the visible and near-ultraviolet regions in neat α- and β-G_n were unsuccessful, and none of the optical micrographs gave patterns that appeared "handed".[26] Still, evidence of helical twisting was obtained by X-ray diffraction from a partially oriented sample of α-G_{10} (vide infra).

X-ray Diffraction Observations. The powder diffraction patterns of nonoriented samples rapidly cooled from the isotropic phase (at >10 °C/min) showed three areas of diffraction: a sharp, low-angle peak (or peaks) (d = 20–50 Å), a mid-angle region peak (6–12 Å) that was not always present, and a broad feature at high angle (d < 6 Å). When the sample was heated to form its isotropic phase, only a broad diffuse peak, typical of liquid alkanes, remained and the optical birefringence disappeared. The isotropic phase patterns (see Figure 3) are typical of a liquid alkane. Representative diffraction patterns for G_{11} and G_{14} are shown in Figure 3. These diffraction characteristics are compatible with either a smectic A or C phase or a columnar phase[27]—but not one with a simple hexagonal packing of columns.[2a,28]

Specific chain conformations of the α anomers, especially, could provide length-to-breadth ratios compatible with biaxial smectic A like phases;[29] some monoalkylated glucopyranosides do give smectic A phases.[7] Alternatively, if the molecules assume a more symmetrical disk shape, a columnar phase should result.[29] Three not mutually exclusive factors can give rise to a diffuse peak in the mid-angle region: undulation of layers in a smectic phase,[30-32] a screw type arrangement of disks, or undulation of columns in a columnar phase.[28]

Molecular Packing: Evidence for Columnar Ordering. Low-angle diffraction, like that observed, is expected from G_n if they adopt discoidal conformations and pack in a columnar arrangement. To obtain more definitive evidence for this packing, diffraction from slowly cooled samples on a single cover glass slide was measured. Unlike the very thin samples sandwiched between two glass plates that displayed monochromatic optical micrographs, several of these slowly cooled thicker materials appeared as multicolored, large, birefringent crosses. Diffraction data from α-G_{10}, β-G_{10}, α-G_{16}, and β-G_{16}, recorded photographically on a Nicolet $P2_1$ diffractometer, are summarized in Table IV: the Polaroid photographs did not reproduce well. Optical microscopy showed that the diffraction pattern of α-G_{16} was totally of the mesophase and that of α-G_{10} was, at least partially, of crystalline material.

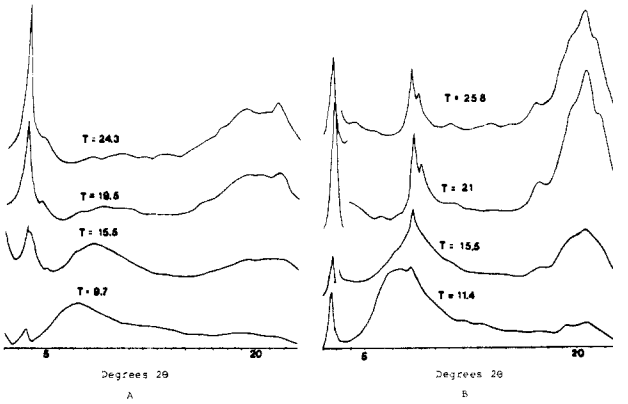

Figure 4. X-ray diffraction patterns of (A) α-G_{10} and (B) β-G_{10} at temperatures (°C) shown.

Most samples gave only annular diffraction. However, the patterns in different orientations were not identical, indicating some preferential ordering. A faint second-order diffraction feature from each sample was observed at approximately twice the diffraction vector of the broad, sometimes structured, high-angle peak. This is strong evidence for the stacking of molecules into columns and allows us to calculate interdisk spacings of 4.5 (1) Å for α-G_{10}, 3.34 (9) Å for α-G_{16}, 3.54 (10) Å for β-G_{10}, and 3.34 (9) Å for β-G_{16}.

One sample of α-G_{10} was especially well aligned, with a diffraction pattern reminiscent of those for flat films of columnar triphenylenehexaylhexa-*n*-dodecanoate.[33] It showed horizontal layer lines (an equatorial, a first, and a weak second layer line) corresponding to a spacing of 4.5 (1) Å. Unlike the other G_n, however, α-G_{10} exhibited multiple reflections along the meridian. The values shown in Table IV are consistent (within our precision limits) with a regular helical stacking of disks for α-G_{10}, such that one helical twist occurs every sixth disk: a rotation of 360°/6 by each disk-shaped molecule, spaced 4.5 (1) Å apart, produces a repeat of 27 (2) Å. The multiple orders of diffraction observed along the meridian compare well with this value.

The diffraction data for the slowly cooled samples, therefore, provide strong evidence that the G_n molecules are disk-shaped in their mesophases and associate in columns. Additionally, in summary, the diffraction data show that disk stacking may be disordered or ordered, depending on the G_n homologue and anomer and its thermal history.

Molecular Packing: Temperature Effects. The effects of temperature on aged α- and β-G_{10} are illustrated in Figure 4. When α- or β-G_{10} was cooled, the intensity of the low-angle and high-angle peaks diminished, while a new peak developed in the mid-angle range. The behavior was reversible. These results show that temperature has a significant influence on the type and degree of ordering in the G_n. At higher temperatures, the columns are better aligned with respect to one another, but molecules within a column are less organized. As temperature is lowered, both anomeric series showed an increased intensity in the mid-angle diffraction region and decreased intensity in the high- and low-

(26) Malthete, J.; Jacques, J.; Tinh, N. H.; Destrade, C. *Nature (London)* **1982**, *298*, 46.
(27) (a) Lehn, J.-M.; Malthete, J.; Levelut, A.-M. *J. Chem. Soc., Chem. Commun.* **1985**, 1794. (b) de Vries, A. *Mol. Cryst. Liq. Cryst.* **1985**, *131*, 125.
(28) Levelut, A.-M., *J. Phys. (Les Ulis, Fr.)* **1979**, *40*, L81.
(29) Chandrasekhar, S. *Philos. Trans. R. Soc. London A* **1983**, *309*, 93.
(30) Pape, E. H. *Mol. Cryst. Liq. Cryst., Lett.* **1985**, *1*, 139.
(31) Hardouin, F.; Levelut, A.-M. *J. Phys. (Les Ulis Fr.)* **1980**, *41*, 41.
(32) Helfrich, W. B. *J. Phys. (Les Ulis, Fr.)* **1979**, *40*, C3-105.
(33) Takabatake, M.; Iwayanagi, S. *Jpn. J. Appl. Phys.* **1982**, *21*, L685.

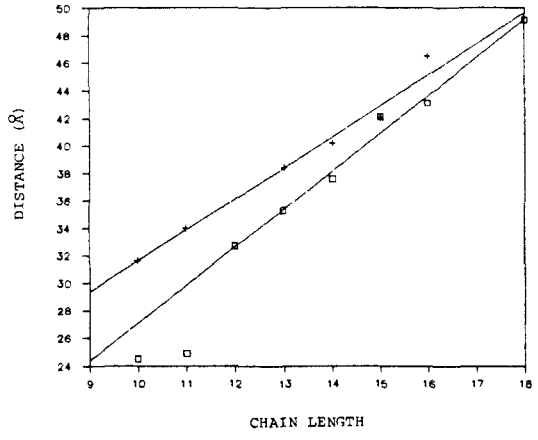

Figure 5. *D* values (calculated from lowest angle peak) vs chain length for G_n samples rapidly cooled from the isotropic phase: α series (□); β series (+).

angle regions. We attribute this to a helically twisted shape of the columns themselves.[26,34,35] An explanation based upon a smectic phase, for which the mid-angle diffuse peak would arise from undulations of the layers, is incompatible with the loss of intensity at high angle.

For a nonoriented sample of α-G_{11}, cooled rapidly from the isotropic phase, a particularly sharp, high-angle peak at 22.2 (1)° 2θ (corresponding to 4.00 (1) Å) was observed. It could be selectively and reproducibly formed or eliminated by raising and lowering the temperature. We hypothesize that this peak derives from ordered stacks of the disks. The 4.00-Å separation, with the 4.5 (1)-Å separation observed for α-G_{10}, indicates that α-G_{10} and α-G_{11} disks stack differently than the higher α-homologues, for which interdisk spacings of about 3.4 Å are calculated.

Molecular Packing: Effects of Chain Length. In Figure 5, the distance, calculated from the lowest angle diffraction peak of bulk samples rapidly cooled to 15 °C, is plotted versus the number of carbons in the substituent chains. If additional methylenes were added in a fully extended conformation, the calculated increase in molecular diameter between any G_n and G_{n+1} would be approximately 2.5 Å.

The slope of 2.67 (15) Å per CH_2 for the α series ($n \geq 12$) representing the increase in d_{obsd} ($d_{obsd} = A \sin(180° - \beta) = A \sin\beta$, where A is the lattice constant and β is the interaxial oblique angle) reflects a rectangular packing of columns. The rectangular lattice results from the more asymmetric shape of the α molecules. The slope for the β series, 2.17 (7) Å per CH_2, is that expected for a hexagonal packing (with $\beta = 120°$, 2.5 sin 120° = 2.2 Å). Although not all the low-angle lines could be indexed in a hexagonal lattice, this does not preclude an almost hexagonal type packing. Alternatively, the smaller slope for the β series could be interpreted as a tilting of the disk-shaped molecules with respect to the columnar axis. If no chain interdigitation were to occur, the intercept from each anomeric series would be equal to the core diameter of the parent glucopyranose molecule (~8 Å). For the β series, the intercept (10.0 (8) Å) and slope are inconsistent with variable interdigitation of chains.

The intercept, 0 (2) Å, for the longer members of the rapidly cooled α series requires explanation. Since the magnitude of the slope is incompatible with tilting, the smaller than expected intercept indicates that the chains are interdigitated to a constant extent for α-G_{12} and larger homologues. Figure 6 provides further evidence that α-G_{10} and α-G_{11} have a different molecular packing arrangement from their longer homologues.

Incubation Effects. DSC measurements clearly demonstrate the acute dependence of phase behavior on prior thermal history of G_n samples. For instance, when α-G_{10} was cooled from its isotropic phase, kept for 33 h at 25 °C or lower, and then heated to 45 °C, an endotherm corresponding to a mesophase–isotropic transition was observed. On the other hand, no endotherm was observed for a sample treated identically, except that the incubation temperature was 28 °C. The endothermicities and peak temperatures of heating transitions obtained by DSC on α-G_{10} samples incubated for different periods at 24 °C demonstrate that the samples must require more than 6 h of incubation to achieve the most ordered state of the mesophase. Samples melted and held at 26 °C developed increasingly better resolved X-ray diffraction patterns over several days. Similar behavior was observed by optical microscopy on thin, sandwiched samples of α-G_{10}: no mesophase formation was evident until samples, cooled several degrees below their phase transition temperature, had remained there for relatively long periods.

As expected from the previous subsection, α-G_{11} behaved very much like α-G_{10}.[6] When a very thin sample of α-G_{11} was incubated at the mesophase–isotropic phase transition temperature (44 °C), it slowly transformed to fibrous bundles of crystals (Figure 6B), mp 47.5–49.0 °C. The mesophase micrograph is shown in Figure 6A. X-ray data for α-G_{11} that was incubated at a temperature just below that for the mesophase–isotropic transition are shown in Figure 7. They complement the OM results and demonstrate unequivocally an increasingly ordered arrangement of molecules with time.

The effects of incubation on a bulk sample of α-G_{11} were most evident in DSC measurements. Heating a sample that had been cooled previously from 47 to 0 °C led to an endotherm (mesophase–isotropic) with $T_{max} > 45$ °C, followed by an *exotherm* (isotropic–crystal) and finally a second endotherm (crystal–isotropic) at ca. 50 °C (see Figure 8A). This requires the formation of a reentrant solid phase.[12] When observed by OM, a sample of very slowly heated α-G_{11} does indeed transform from mesophase to isotropic liquid to solid and then to isotropic liquid. If cooled from 70 to 47 °C and then incubated there for 10 h, the material remained isotropic; subsequent cooling to 0 °C led to a "normal" exotherm (isotropic–mesophase); the heating cycle from 0 °C displayed both endotherms and the intermediate exotherm. When cooled from 70 to 35 °C (i.e., below the mesophase–isotropic phase transition) and incubated there for 10 h, the material was transformed to almost pure crystal: heating gave rise to a small exotherm for solidification of the isotropic liquid derived from melting of residual mesophase and a very large endotherm for the crystal–isotropic transition (Figure 8B).

From these results, we conclude that the molecules orient in several consecutive steps that are temperature and time dependent. Apparently, crystal cannot be formed from isotropic α-G_{11} unless some mesophase is present, just as mesophase does not form without some prior ordering in its supercooled isotropic phase.

The shorter β anomers behave in a somewhat similar fashion, although no exotherm in the heating curve was observed. When a thin sample of β-G_{11} was incubated for 1 day at a temperature at or just below that for the mesophase–isotropic phase transition, starlike bundles of fibrous crystals that melted at 47.5–48.0 °C slowly formed. The mesophase texture is shown in Figure 6C.

The textures of the optical micrographs are distinctive in each anomeric series: small Maltese crosses occur in the β series and larger patterns are seen, regardless of incubation time, in the α series. Several representative micrographs are collected in Figure 6. Assignment of 6D and 6F, especially, to mesophase requires some explanation since the micrographs appear somewhat crystalline. The major evidence is that the patterns disappeared when the crossed polarizers of the microscope were turned parallel. That and the X-ray observations on samples similarly treated, which lacked the sharp diffraction peaks diagnostic of crystalline material, led to the phase assignments.

In both the α- and β-anomeric series, the higher homologues gave no evidence for reentrant phases by DSC or optical microscopy. We attribute this difference to the much greater viscosity of the longer chained G_n, rather than an intrinsic change in the phase behavior. Crystallization is promoted when the samples are ordered but are not so viscous (as at room temper-

(34) Levelut, A.-M. *J. Chim. Phys.* **1983**, *80*, 149.
(35) (a) Safinya, C. R.; Clark, N. A.; Liang, K. S.; Varady, W. A.; Chiang, L. Y. *Mol. Cryst. Liq. Cryst.* **1985**, *123*, 205. (b) Tsykalo, A. L. *Mol. Cryst. Liq. Cryst.* **1985**, *128*, 99.

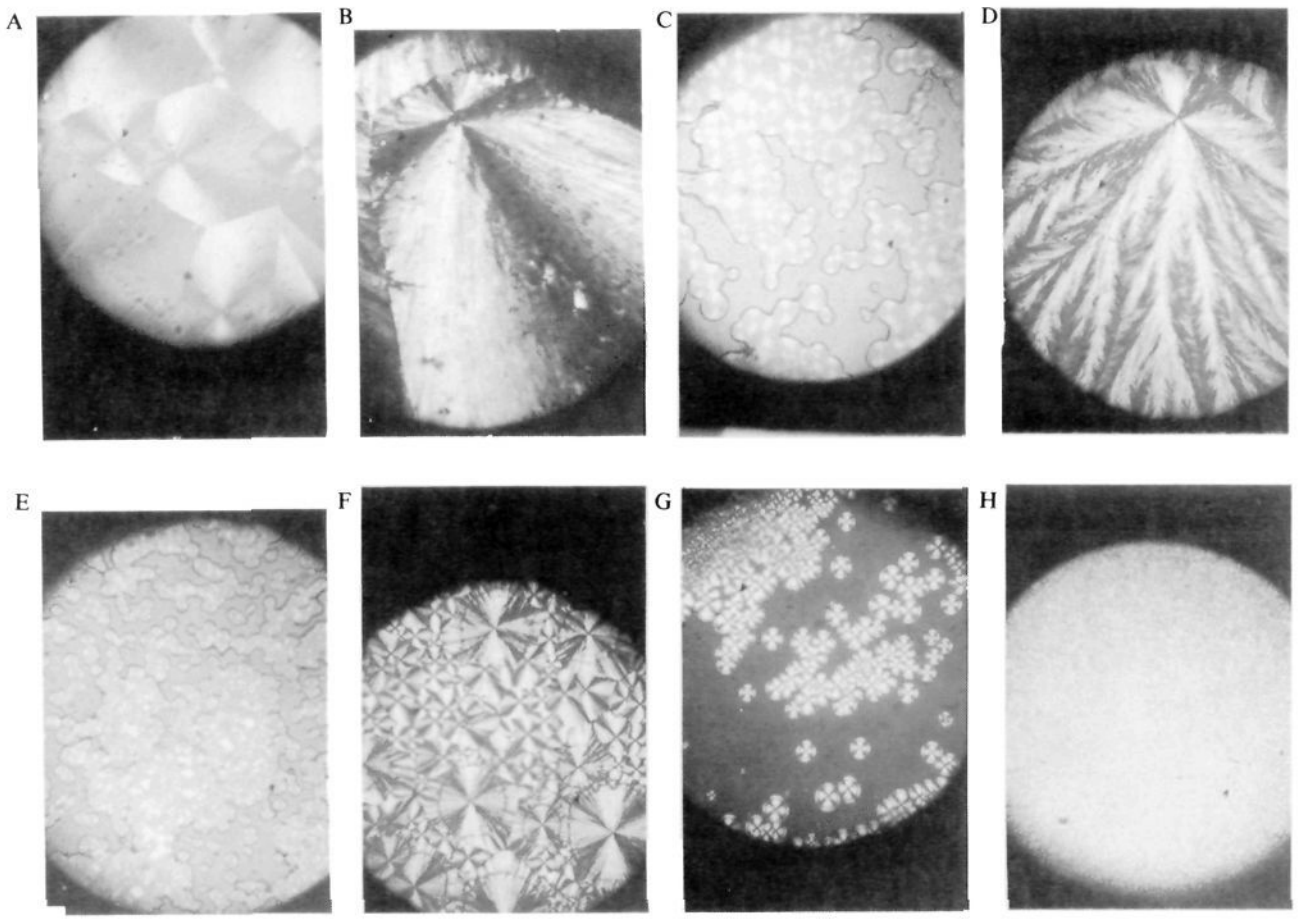

Figure 6. Optical textures of G_n observed through crossed polarizers. (A) α-G_{11} mesophase; cooled very slowly (<1 °C/min) from isotropic and aged for 1 day at 26 °C; ×45. (B) α-G_{11} crystal; incubated for 1 day at 44 °C; ×45. (C) β-G_{11} mesophase; cooled very slowly (<0.5 °C/min) from isotropic to 38 °C; ×45. (D) α-G_{16} mesophase; cooled very slowly (<0.5 °C/min) from isotropic to 58 °C; ×45. (E) β-G_{16} mesophase; cooled very slowly (<1 °C/min) from isotropic and aged several days at 26 °C; ×45. (F) α-G_{18} mesophase; cooled very slowly (<1 °C/min) from isotropic and aged for 1 day at 26 °C; ×45. (G) α-G_{18} mesophase growing in isotropic liquid; cooled slowly (<2 °C/min) from isotropic to 57.5 °C; ×45. (H) β-G_{18} mesophase; cooled rapidly (>20 °C/min) from isotropic to room temperature; ×45. The telescope magnification at which patterns were photographed is ×100; photographs have been reduced to 45% of their original size.

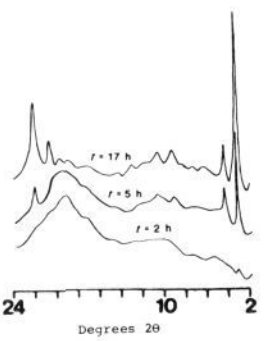

Figure 7. X-ray diffraction patterns of an α-G_{11} sample heated to 50 °C, slowly cooled to 47 °C, and incubated there for the lengths of time shown.

ature) to preclude the motions necessary to permit further ordering.

Heating and Cooling Rate Effects. Substantial supercooling effects were observed by DSC and X-ray diffraction measurements. Thus, upon slow (0.5 °C/min) cooling from the isotropic phase, the exotherm observed was 15–20 °C below the peak temperature of the heating endotherm for the α series, but less than 10 °C for the β series. In general, T_{max} and ΔH, the heat of transition, decreased as the cooling rate increased. For α-G_{11}, cooling from 55 °C at 0.1, 0.5, and 10 °C/min led to exotherms with T_{max} (and ΔH in J/g) of 35.6 °C (–80.2), 29.2 °C (–75.7), and 15.6 °C (–71.7), respectively. Heating these cooled samples from 0 °C led to histograms similar to Figure 8. Both mesophase and crystalline material were present. Rapid cooling (or no in-

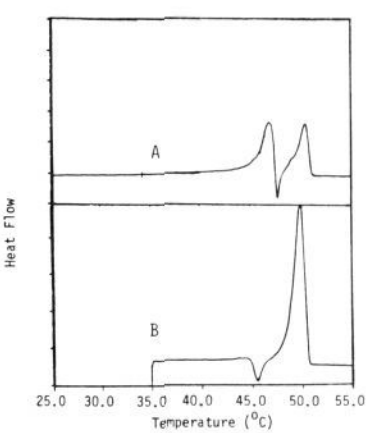

Figure 8. DSC heating cycles of α-G_{11} from 0 to 55 °C (>25 °C shown) (A) immediately after being cooled from the isotropic phase at 0.5 °C/min and (B) from 35 to 55 °C after incubating at 35 °C for 10 h. Note the increased amount of crystalline material in (B) represented by the endotherm near 50 °C.

cubation) produced little crystalline material, whereas slow cooling (or lengthy incubation) increased the fraction of crystalline material. The heating histograms also depend upon the rate of heating of samples that had been cooled in the same way from 70 to 0 °C. The most rapid heating rate yielded a very broad endotherm that approximates a temperature-distorted mesophase–isotropic transition. The more slowly heated samples

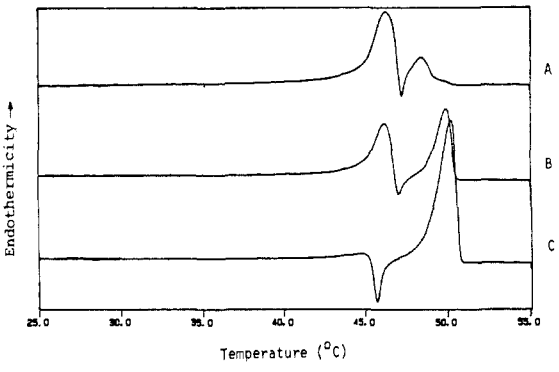

Figure 9. DSC curves of α-G_{11} cooled at 0.5 °C/min illustrating the effects of heating rate on the relative proportions and type of material in the mesophase (near 45 °C) and crystalline phase (near 50 °C). Heating rates were (A) 10, (B) 0.5, and (C) 0.1 °C/min.

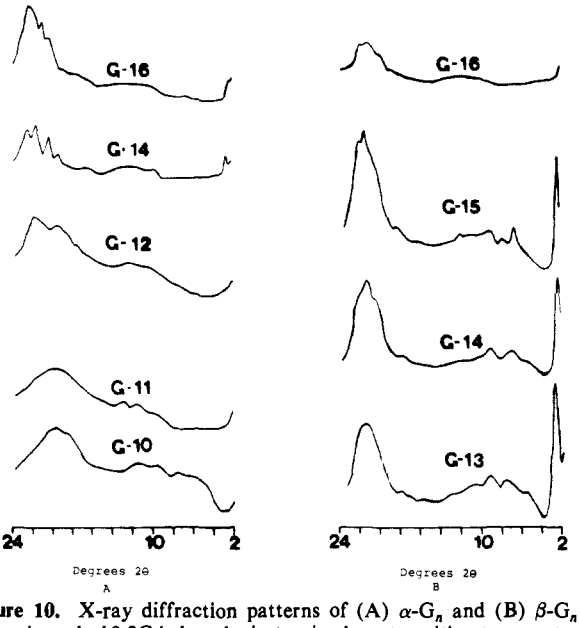

Figure 10. X-ray diffraction patterns of (A) α-G_n and (B) β-G_n at approximately 10 °C below the isotropic phase transition temperatures.

showed an exotherm characteristic of the crystallization of isotropic material (Figure 9).

The influence of heating and cooling rates on the phase transition temperatures diminished with increasing length of the acyl chains on the α- and β-G_n. We attribute this to the increased viscosity of the longer chained compounds. Several of them, when incubated for long periods, undergo small changes in both their phase transition temperatures and heats of transition (see Incubation section).

In addition, in the X-ray diffraction patterns, little or no low-angle peak is seen for samples of α anomers cooled slowly to just below their isotropic transition and held there for less than 30 min. Similarly treated β anomers do show an intense low-angle peak (Figure 10; compare with Figure 3, where both anomeric series show peaks at low angle for samples cooled rapidly to 15 °C). From this, we deduce that β anomers are able to organize themselves into columns more easily.

Rapidly cooled bulk samples of α-G_{16}, which give intense peaks at low angle, show only a broad diffraction feature in the high-angle region (Figure 11A) indicative of no order among disk-shaped molecules within the column. This pattern is consistent with a rectangular disordered columnar phase type (D_{rd} in Destrade's terminology[36]), while the more structured high-angle features in the patterns obtained for the slowly cooled incubated

(36) Destrade, C.; Tinh, N.-H.; Gasparoux, H.; Malthete, J.; Levelut, A.-M. *Mol. Cryst. Liq. Cryst.* **1981**, *71*, 111.

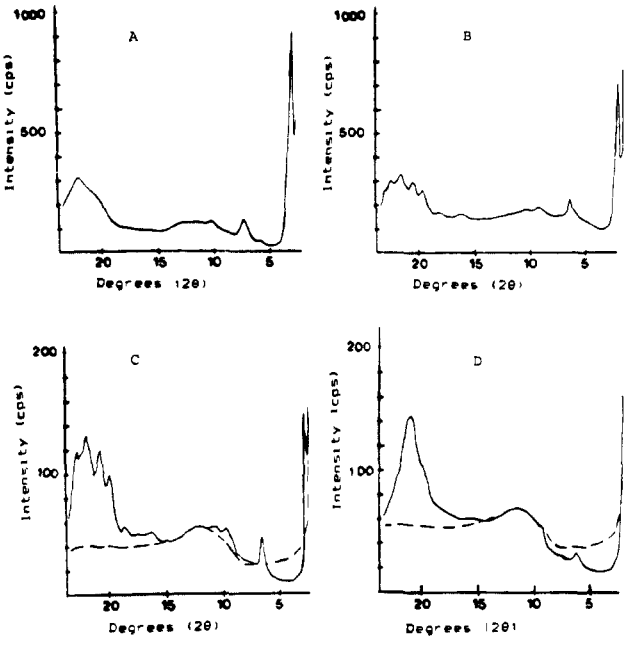

Figure 11. Powder diffraction patterns of α-G_{16}. (A) A quickly cooled bulk sample; (B) a slowly cooled bulk sample; (C) a slowly cooled, partially oriented, thin sample on a cover glass; (D) a quickly cooled, partially oriented, thin sample on a cover glass. To improve signal-to-noise, patterns C and D were recorded at 0.25° 2θ/min. Patterns A and B were recorded at 1° 2θ/min. Dashed lines in C and D represent patterns obtained from the cover glass alone.

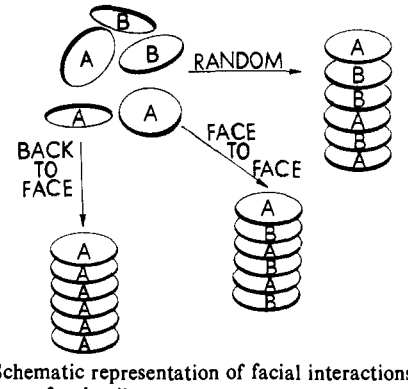

Figure 12. Schematic representation of facial interactions possible for the G_n. See text for details.

bulk samples (Figure 11B), as well as the slowly cooled thin samples (Figure 11C), are of the rectangular ordered columnar phase type (D_{rd}). Finally, the thin samples, with relatively more nucleation sites, are less susceptible to supercooling than the thick ones. Thus, much smaller columnar domains form upon fast cooling, and little or no intensity is observed at low angle (Figure 11D).

Optical micrographs of rapidly cooled (>10 °C/min) thin samples of α- and β-G_n sandwiched between glass plates showed mosaic patterns, such as in Figure 6F (that resemble shards of patterns in 6A and 6E obtained from slower cooling).

Conclusions

The data presented clearly demonstrate the complexity associated with identification of the α- and β-G_n mesophases: both molecular structure, prior thermal history, and sample thickness appear to be important factors. Since other discotic molecules have not been reported to include such complexity, its source must be related to the chirality and asymmetry of the glucopyranose cores.

A symmetrical, achiral, discotic molecule with n chains has identical faces and an n-fold axis of symmetry perpendicular to the core plane. Therefore, the face with which individual molecules stack initially and their rotational orientations within a forming

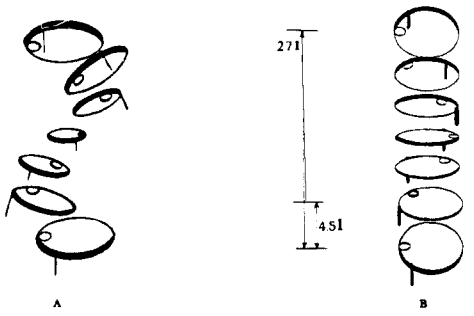

Figure 13. (A) Schematic diagram of the sheared helical arrangement assumed by α-G_{10} molecules at lower temperatures as a result of the initially axial chain. (b) Schematic diagram of the helically arranged α-G_{10} molecules stacked perpendicularly to the column axis at higher temperatures leading to better columnar ordering.

column have little consequence with regard to overall phase order. This is not the case with G_n. Each face of a G_n molecule is chiral and diastereotopic with respect to the faces of another (equivalent) G_n; the cores possess no nontrivial axes of symmetry. Thus, as shown in Figure 12, stacks may include A–A + B–B packing, A–B packing, or random facial packing. Within each facial packing mode, the molecules may be rotationally disorganized or organized in several different fashions. At this time, we do not know which mode(s) is preferred. However, we suspect that the lowest energy arrangement is not random with respect to facial or chain packing and that the thermal and temporal dependencies of samples on their phase morphologies is a consequence of less preferred packing arrangements being "trapped" when isotropic samples are supercooled to mesophase temperatures. Some orientations may lead to mesophases and others to crystals. Considering the complexity of movement, it is reasonable to assume that rotational reorganization of chains (and cores) within a column is more facile than interfacial reorganization or disk flipping. Thus, molecular assemblies of some G_n, trapped in monotropic mesophases for very long periods, can be crystallized relatively rapidly by increasing the temperature to above the mesophase–isotropic transition temperature but below the crystal–isotropic transition temperature. Since crystallization of neat G_n requires preliminary intermolecular arrangements (as provided by the mesophases), the crystal is not available directly from cooling the isotropic phase.

The molecules studied behaved as three subgroups: the short-chained α-G_n, the longer chain α-G_n, and the β-G_n. The facial asymmetry is greater in the α series due to its one axial chain. It is particularly emphasized for the shorter chained α-G_{10} and α-G_{11}, for which several important differences are observed when compared with their higher homologues: (1) the intercolumnar and interdisk distances indicate different packing arrangements; (2) the shorter α-G_n form reentrant solid phases and tend to crystallize slowly at room temperature, whereas we have not observed crystallinity in the higher homologues; (3) the transition enthalpies of the shorter α-G_n do not follow the trend established by the higher homologues.

The reason the α-G_n ($n \geq 12$) pack differently than α-G_{10} and α-G_{11} may be a consequence of interchain and intercore energetics. The most unsymmetrical G_n, α-G_{10}, gave the best aligned sample for X-ray diffraction studies. Indeed, the α series, in general, formed the largest monodomains observed by OM and x-ray diffraction. A large degree of asymmetry may cause deeper intermolecular potential wells to exist, or (in physical terms) specific positions into which the molecules strongly prefer to exist: mesophases from the α series should be more entropically demanding than those from the β series. From the diffraction data we suggest that the α-G_{10} (and probably the α-G_{11}) molecules prefer to organize themselves into helical stacks in which the axially attached chains sit over ring ether oxygens, such that each molecule is rotated (on average) by 60° with respect to its intracolumnar neighbors. Upon cooling, the stacks shrink, creating a tilting of disk planes with respect to one another and producing a twist in the columns themselves (see Figure 13). Loss of columnar alignment, as evidenced by the X-ray diffraction studies, is a consequence of twisting (Figure 4).

As the chains of α-G_n lengthen, we expect that their van der Waals interactions will become more important than core–core considerations, even those due to ratcheting. In fact, the α-anomeric chain, beyond the ester group, can be projected easily along a direction roughly coplanar with the core of a neighboring molecule. The increased importance of the longer chains is seen, however, in the lack of reentrant behavior of the higher homologues. For the shorter G_n, the free energy of activation required to organize the chains of the mesophase into a crystalline arrangement is less than the energy of the mesophase–isotropic transition; thus, reentrant solid phases are observed upon slow heating.

For the longer homologues, the mesophase may no longer be monotropic. In either case, insufficient free energy of activation is available for the crystalline phase to be organized from either an isotropic phase (reentrant behavior) or the mesophase within the time of the experiments.

Both molecular models and our experimental data indicate that the sensitivity of assemblies to facial and rotational packing is less severe in the β series than in the α. The β-G_n can splay their five chains in directions that are within the rough plane defined by the β-glucopyranoside core. All five substituents are equatorial in the chair conformation of the ring. Thus, "ratcheting" is not expected within columns for the β series of mesophases and it is not observed.

Although we are unable at this time to explain all of the phenomena observed with the G_n, the hypotheses included here seem consistent with the principal observations. There is no reason to believe that this comportment is unique to G_n. Other asymmetrically cored discotic molecules should exhibit at least some of the complexities shown by the G_n and, perhaps, some others that the G_n do not show. Since other monosaccharide and disaccharide cores form discotic mesophases,[6] the possibilities for future experimentation and for the creation of anisotropic solvents with uniquely tailored molecular packing arrangements are manifold.

Note Added in Proof. The α-G_{16} and α-G_{18} were examined with the National Bureau of Standards small-angle X-ray scattering facility. The accuracy of measurements made and the absence of diffraction features at angles below those accessible on the Picker powder diffractometer were established.

Acknowledgment. We thank Dr. Niel Glaudemans of the National Institutes of Health for the use of his polarimeter, Dr. Ray Baughman of Allied Corp. for some preliminary differential scanning calorimetry measurements, and Dr. Ray Butcher of Howard University for use of his Nicolet $P2_1$ diffractometer to collect the two-dimensional X-ray photographs. R.G.W. acknowledges the National Science Foundation (Grants CHE83-01776 and CHE85-017632) and the Office of Naval Research for financial support. R.G.Z. and N.L.M. are grateful for a NATO postdoctoral travel fellowship and an ARCS scholarship, respectively. Messrs. Ali Nami and Jon Baldvins prepared samples of several α- and β-G_n and recorded the NMR spectra. We are grateful to Dr. Charles Han and Dr. John Barnes for their assistance with the SAXS experiment.

Registry No. α-G_{10}, 73837-96-4; α-G_{11}, 113008-28-9; α-G_{12}, 112988-55-3; α-G_{13}, 112988-56-4; α-G_{14}, 112988-57-5; α-G_{15}, 112988-58-6; α-G_{16}, 73827-58-4; α-G_{18}, 73827-59-5; β-G_{10}, 99422-57-8; β-G_{11}, 112988-59-7; β-G_{12}, 112988-60-0; β-G_{13}, 112988-61-1; β-G_{14}, 113008-29-0; β-G_{15}, 112988-62-2; β-G_{16}, 99422-58-9; β-G_{18}, 112988-63-3.